Supplement of Biogeosciences, 18, 1803–1822, 2021
https://doi.org/10.5194/bg-18-1803-2021-supplement

Biogeosciences
Open Access

Supplement of

An observation-based evaluation and ranking of historical Earth system model simulations in the northwest North Atlantic Ocean

Arnaud Laurent et al.

Correspondence to: Arnaud Laurent (arnaud.laurent@dal.ca)

S1 Introduction

This supporting information provides the equations for the biogeochemical model and additional Tables S1 to S3 and Figures S1 to S14 for the main article.

S2 Biogeochemical model

The model has 10 state variables, namely phytoplankton, split into small (P_S) and large (P_L) size groups with their respective chlorophyll concentration (Chl_S and Chl_L), zooplankton, divided into 2 size classes representing the micro- (Z_S) and meso- (Z_L) zooplankton, nitrate (NO_3^-), ammonium (NH_4^+), and small (D_S) and large (D_L) detritus. State variables are in mmol N m^{-3} except for chlorophyll (mg m^{-3}).

The time rates of change of the biogeochemical state variables due to biological processes are described below. The list of parameters, values and units is presented in Table S1.

$$\frac{\partial \mathrm{P_S}}{\partial t} = \mu_{\mathrm{P_S}}^{\max} L_{\mathrm{P_S}}^{\mathrm{E}} L_{\mathrm{P_S}}^{\mathrm{N}} \mathrm{P_S} - g_{\mathrm{Z_S P_S}}^{\max} \frac{\mathrm{P_S^2}}{k_{\mathrm{Z_S P_S}} + \mathrm{P_S^2}} \mathrm{Z_S} - g_{\mathrm{Z_L P_S}}^{\max} \frac{\mathrm{P_S^2}}{k_{\mathrm{Z_L P_S}} + \mathrm{P_S^2}} e^{-\psi_{\mathrm{Z_L P_S}}(\mathrm{P_L}+\mathrm{Z_S})} \mathrm{Z_L} - m_{\mathrm{P_S}} \mathrm{P_S} - w_{\mathrm{P_S}} \frac{\partial \mathrm{P_S}}{\partial z} \tag{1}$$

$$\begin{aligned}\frac{\partial \mathrm{P_L}}{\partial t} = {} & \mu_{\mathrm{P_L}}^{\max} L_{\mathrm{P_L}}^{\mathrm{E}} L_{\mathrm{P_L}}^{\mathrm{N}} \mathrm{P_L} - g_{\mathrm{Z_S P_L}}^{\max} \frac{\mathrm{P_L^2}}{k_{\mathrm{Z_S P_L}} + \mathrm{P_L^2}} e^{-\psi_{\mathrm{Z_S P_L}} \mathrm{P_S}} \mathrm{Z_S} - g_{\mathrm{Z_L P_L}}^{\max} \frac{\mathrm{P_L^2}}{k_{\mathrm{Z_L P_L}} + \mathrm{P_L^2}} \mathrm{Z_L} - m_{\mathrm{P_L}} \mathrm{P_L} \\ & - \tau(\mathrm{D_S} + \mathrm{P_L}) \mathrm{P_L} - w_{\mathrm{P_L}} \frac{\partial \mathrm{P_L}}{\partial z}\end{aligned} \tag{2}$$

$$\begin{aligned}\frac{\partial \mathrm{Chl_S}}{\partial t} = {} & \rho_{\mathrm{Chl}} \mu_{\mathrm{P_S}}^{\max} L_{\mathrm{P_S}}^{\mathrm{E}} L_{\mathrm{P_S}}^{\mathrm{N}} \mathrm{Chl_S} - \frac{\mathrm{Chl_S}}{\mathrm{P_S}} \left(g_{\mathrm{Z_S P_S}}^{\max} \frac{\mathrm{P_S^2}}{k_{\mathrm{Z_S P_S}} + \mathrm{P_S^2}} \mathrm{Z_S} + g_{\mathrm{Z_L P_S}}^{\max} \frac{\mathrm{P_S^2}}{k_{\mathrm{Z_L P_S}} + \mathrm{P_S^2}} e^{-\psi_{\mathrm{Z_L P_S}}(\mathrm{P_L}+\mathrm{Z_S})} \mathrm{Z_L} \right) \\ & - m_{\mathrm{P_S}} \mathrm{Chl_S} - w_{\mathrm{P_S}} \frac{\partial \mathrm{Chl_S}}{\partial z}\end{aligned} \tag{3}$$

$$\begin{aligned}\frac{\partial \mathrm{Chl_L}}{\partial t} = {} & \rho_{\mathrm{Chl}} \mu_{\mathrm{P_L}}^{\max} L_{\mathrm{P_L}}^{\mathrm{E}} L_{\mathrm{P_L}}^{\mathrm{N}} \mathrm{Chl_L} - \frac{\mathrm{Chl_L}}{\mathrm{P_L}} \left(g_{\mathrm{Z_S P_L}}^{\max} \frac{\mathrm{P_L^2}}{k_{\mathrm{Z_S P_L}} + \mathrm{P_L^2}} e^{-\psi_{\mathrm{Z_S P_L}} \mathrm{P_S}} \mathrm{Z_S} + g_{\mathrm{Z_L P_L}}^{\max} \frac{\mathrm{P_L^2}}{k_{\mathrm{Z_L P_L}} + \mathrm{P_L^2}} \mathrm{Z_L} \right) \\ & - m_{\mathrm{P_L}} \mathrm{Chl_L} - \tau(\mathrm{D_S} + \mathrm{P_L}) \mathrm{Chl_L} - w_{\mathrm{P_L}} \frac{\partial \mathrm{Chl_L}}{\partial z}\end{aligned} \tag{4}$$

$$\begin{aligned}\frac{\partial \mathrm{Z_S}}{\partial t} = {} & \Bigg(\left(g_{\mathrm{Z_S P_S}}^{\max} \frac{\mathrm{P_S^2}}{k_{\mathrm{Z_S P_S}} + \mathrm{P_S^2}} + g_{\mathrm{Z_S P_L}}^{\max} \frac{\mathrm{P_L^2}}{k_{\mathrm{Z_S P_L}} + \mathrm{P_L^2}} e^{-\psi_{\mathrm{Z_S P_L}} \mathrm{P_S}} \right) \beta_{\mathrm{Z_S}} - l_{\mathrm{Z_S}}^{\mathrm{BM}} \\ & - l_{\mathrm{Z_S}}^{\mathrm{E}} \left(\frac{\mathrm{P_S^2}}{k_{\mathrm{Z_S P_S}} + \mathrm{P_S^2}} + \frac{\mathrm{P_L^2}}{k_{\mathrm{Z_S P_L}} + \mathrm{P_L^2}} e^{-\psi_{\mathrm{Z_S P_L}} \mathrm{P_S}} \right) \beta_{\mathrm{Z_S}} - m_{\mathrm{Z_S}} \mathrm{Z_S} \Bigg) \mathrm{Z_S} - g_{\mathrm{Z_L Z_S}}^{\max} \frac{\mathrm{Z_S^2}}{k_{\mathrm{Z_L Z_S}} + \mathrm{Z_S^2}} \mathrm{Z_L}\end{aligned} \tag{5}$$

$$\frac{\partial \mathrm{Z_L}}{\partial t} = \Bigg(\Bigg(g_{\mathrm{Z_LP_S}}^{\max}\frac{\mathrm{P_S^2}}{k_{\mathrm{Z_LP_S}}+\mathrm{P_S^2}}e^{-\psi_{\mathrm{Z_LP_S}}(\mathrm{P_L}+\mathrm{Z_S})} + g_{\mathrm{Z_LP_L}}^{\max}\frac{\mathrm{P_L^2}}{k_{\mathrm{Z_LP_L}}+\mathrm{P_L^2}} + g_{\mathrm{Z_LZ_S}}^{\max}\frac{\mathrm{Z_S^2}}{k_{\mathrm{Z_LZ_S}}+\mathrm{Z_S^2}}\Bigg)\beta_{\mathrm{Z_L}} \\ - l_{\mathrm{Z_L}}^{\mathrm{BM}} - l_{\mathrm{Z_L}}^{\mathrm{E}}\Bigg(\frac{\mathrm{P_S^2}}{k_{\mathrm{Z_LP_S}}+\mathrm{P_S^2}}e^{-\psi_{\mathrm{Z_LP_S}}(\mathrm{P_L}+\mathrm{Z_S})} + \frac{\mathrm{P_L^2}}{k_{\mathrm{Z_LP_L}}+\mathrm{P_L^2}} + \frac{\mathrm{Z_S^2}}{k_{\mathrm{Z_LZ_S}}+\mathrm{Z_S^2}}\Bigg)\beta_{\mathrm{Z_L}} - m_{\mathrm{Z_L}}\mathrm{Z_L}\Bigg)\mathrm{Z_L} \tag{6}$$

$$\frac{\partial \mathrm{NO_3^-}}{\partial t} = -\mu_{\mathrm{P_S}}^{\max}L_{\mathrm{P_S}}^{\mathrm{E}}L_{\mathrm{P_S}}^{\mathrm{NO_3^-}}\mathrm{P_S} - \mu_{\mathrm{P_L}}^{\max}L_{\mathrm{P_L}}^{\mathrm{E}}L_{\mathrm{P_L}}^{\mathrm{NO_3^-}}\mathrm{P_L} + \hat{n}\mathrm{NH_4^+} \tag{7}$$

$$\frac{\partial \mathrm{NH_4^+}}{\partial t} = -\mu_{\mathrm{P_S}}^{\max}L_{\mathrm{P_S}}^{\mathrm{E}}L_{\mathrm{P_S}}^{\mathrm{NH_4^+}}\mathrm{P_S} - \mu_{\mathrm{P_L}}^{\max}L_{\mathrm{P_L}}^{\mathrm{E}}L_{\mathrm{P_L}}^{\mathrm{NH_4^+}}\mathrm{P_L} - \hat{n}\mathrm{NH_4^+} + l_{\mathrm{Z_S}}^{\mathrm{BM}}\mathrm{Z_S} + l_{\mathrm{Z_L}}^{\mathrm{BM}}\mathrm{Z_L} \\ + l_{\mathrm{Z_S}}^{\mathrm{E}}\Bigg(\frac{\mathrm{P_S^2}}{k_{\mathrm{Z_SP_S}}+\mathrm{P_S^2}} + \frac{\mathrm{P_L^2}}{k_{\mathrm{Z_SP_L}}+\mathrm{P_L^2}}e^{-\psi_{\mathrm{Z_SP_L}}\mathrm{P_S}}\Bigg)\beta_{\mathrm{Z_S}}\mathrm{Z_S} + l_{\mathrm{Z_L}}^{\mathrm{E}}\Bigg(\frac{\mathrm{P_S^2}}{k_{\mathrm{Z_LP_S}}+\mathrm{P_S^2}}e^{-\psi_{\mathrm{Z_LP_S}}(\mathrm{P_L}+\mathrm{Z_S})} \\ + \frac{\mathrm{P_L^2}}{k_{\mathrm{Z_LP_L}}+\mathrm{P_L^2}} + \frac{\mathrm{Z_S^2}}{k_{\mathrm{Z_LZ_S}}+\mathrm{Z_S^2}}\Bigg)\beta_{\mathrm{Z_L}}\mathrm{Z_L} + \hat{r}_{\mathrm{D_S}}\mathrm{D_S} + \hat{r}_{\mathrm{D_L}}\mathrm{D_L} \tag{8}$$

$$\frac{\partial \mathrm{D_S}}{\partial t} = \Bigg(g_{\mathrm{Z_SP_S}}^{\max}\frac{\mathrm{P_S^2}}{k_{\mathrm{Z_SP_S}}+\mathrm{P_S^2}} + g_{\mathrm{Z_SP_L}}^{\max}\frac{\mathrm{P_L^2}}{k_{\mathrm{Z_SP_L}}+\mathrm{P_L^2}}e^{-\psi_{\mathrm{Z_SP_L}}\mathrm{P_S}}\Bigg)(1-\beta_{\mathrm{Z_S}})\mathrm{Z_S} \\ + \Bigg(g_{\mathrm{Z_LP_S}}^{\max}\frac{\mathrm{P_S^2}}{k_{\mathrm{Z_LP_S}}+\mathrm{P_S^2}}e^{-\psi_{\mathrm{Z_LP_S}}(\mathrm{P_L}+\mathrm{Z_S})} + g_{\mathrm{Z_LP_L}}^{\max}\frac{\mathrm{P_L^2}}{k_{\mathrm{Z_LP_L}}+\mathrm{P_L^2}} + g_{\mathrm{Z_LZ_S}}^{\max}\frac{\mathrm{Z_S^2}}{k_{\mathrm{Z_LZ_S}}+\mathrm{Z_S^2}}\Bigg)(1-\beta_{\mathrm{Z_L}})\mathrm{Z_L} + m_{\mathrm{P_S}}\mathrm{P_S} \\ + m_{\mathrm{P_L}}\mathrm{P_L} + m_{\mathrm{Z_S}}\mathrm{Z_S^2} - \hat{r}_{\mathrm{D_S}}\mathrm{D_S} - \tau(\mathrm{D_S}+\mathrm{P_L})\mathrm{D_S} - w_{\mathrm{D_S}}\frac{\partial \mathrm{D_S}}{\partial z} \tag{9}$$

$$\frac{\partial \mathrm{D_L}}{\partial t} = \tau(\mathrm{D_S}+\mathrm{P_L})^2 + m_{\mathrm{Z_L}}\mathrm{Z_L^2} - \hat{r}_{\mathrm{D_L}}\mathrm{D_L} - w_{\mathrm{D_L}}\frac{\partial \mathrm{D_L}}{\partial z} \tag{10}$$

$$\frac{\partial \mathrm{O_2}}{\partial t} = \mu_{\mathrm{P_S}}^{\max}L_{\mathrm{P_S}}^{\mathrm{E}}\Bigg(\frac{L_{\mathrm{P_S}}^{\mathrm{NO_3^-}}}{L_{\mathrm{P_S}}^{\mathrm{N}}}R_{\mathrm{O_2:NO_3^-}} + \frac{L_{\mathrm{P_S}}^{\mathrm{NH_4^+}}}{L_{\mathrm{P_S}}^{\mathrm{N}}}R_{\mathrm{O_2:NH_4^+}}\Bigg)L_{\mathrm{P_S}}^{\mathrm{N}}\mathrm{P_S} + \mu_{\mathrm{P_S}}^{\max}L_{\mathrm{P_S}}^{\mathrm{E}}\Bigg(\frac{L_{\mathrm{P_L}}^{\mathrm{NO_3^-}}}{L_{\mathrm{P_L}}^{\mathrm{N}}}R_{\mathrm{O_2:NO_3^-}} \\ + \frac{L_{\mathrm{P_L}}^{\mathrm{NH_4^+}}}{L_{\mathrm{P_L}}^{\mathrm{N}}}R_{\mathrm{O_2:NH_4^+}}\Bigg)L_{\mathrm{P_L}}^{\mathrm{N}}\mathrm{P_L} - 2\hat{n}\mathrm{NH_4^+} - R_{\mathrm{O_2:NH_4^+}}\Bigg(l_{\mathrm{Z_S}}^{\mathrm{BM}}\mathrm{Z_S} + l_{\mathrm{Z_L}}^{\mathrm{BM}}\mathrm{Z_L} + l_{\mathrm{Z_S}}^{\mathrm{E}}\Bigg(\frac{\mathrm{P_S^2}}{k_{\mathrm{Z_SP_S}}+\mathrm{P_S^2}} \\ + \frac{\mathrm{P_L^2}}{k_{\mathrm{Z_SP_L}}+\mathrm{P_L^2}}e^{-\psi_{\mathrm{Z_SP_L}}\mathrm{P_S}}\Bigg)\beta_{\mathrm{Z_S}}\mathrm{Z_S} + l_{\mathrm{Z_L}}^{\mathrm{E}}\Bigg(\frac{\mathrm{P_S^2}}{k_{\mathrm{Z_LP_S}}+\mathrm{P_S^2}}e^{-\psi_{\mathrm{Z_LP_S}}(\mathrm{P_L}+\mathrm{Z_S})} + \frac{\mathrm{P_L^2}}{k_{\mathrm{Z_LP_L}}+\mathrm{P_L^2}} \\ + \frac{\mathrm{Z_S^2}}{k_{\mathrm{Z_LZ_S}}+\mathrm{Z_S^2}}\Bigg)\beta_{\mathrm{Z_L}}\mathrm{Z_L} + \hat{r}_{\mathrm{D_S}}\mathrm{D_S} + \hat{r}_{\mathrm{D_L}}\mathrm{D_L}\Bigg) \tag{11}$$

Phytoplankton growth is limited by temperature (*T*; °C), light (*E*; W m^{-2}) and nitrogen (N). The maximum growth rate of phytoplankton ($\mu_{\mathrm{P_X}}^{\max}$; d^{-1}) depends on temperature according to *Eppley* [1972]:

$$\mu_{\mathrm{P_X}}^{\max} = \mu_{\mathrm{P_X}}^{0} \cdot \mathrm{Q}^{T}, \tag{12}$$

where $\mu_{P_X}^0$ is the phytoplankton (P_S or P_L) maximum growth rate at 0°C and $Q^T = 0.59 \cdot 1.066^T$. Q^T is also applied to phytoplankton and zooplankton mortality (m_P and m_Z), grazing (g_Z) and zooplankton basal metabolism (l_{BM}) and excretion (l_E).

Light limitation $L_{P_X}^E$ is formulated with an instantaneous growth rate vs. light function (Evans and Parslow, 1985):

$$L_{P_X}^E = \frac{\alpha_{P_X} E}{\sqrt{(\mu_{P_X}^{max})^2 + (\alpha_{P_X})^2 E^2}} , \tag{13}$$

where E is the light intensity (W m^{-2}) and α_{P_X} is the initial slope of the instantaneous growth rate vs light curve for P_S or P_L.

Nutrient limitation factors $L_{P_X}^{NO_3^-}$ and $L_{P_X}^{NH_4^+}$ are calculated similarly for P_S and P_L such that:

$$L_{P_X}^{NO_3^-} = \frac{NO_3^-}{k_{NO_3^-} + NO_3^-} \cdot \frac{1}{1 + NH_4^+/k_{NH_4^+}} \tag{14}$$

$$L_{P_X}^{NH_4^+} = \frac{NH_4^+}{k_{NH_4^+} + NH_4^+} \tag{15}$$

$$L_{P_X}^N = L_{P_X}^{NO_3^-} + L_{P_X}^{NH_4^+} \tag{16}$$

Phytoplankton acclimates to light and nutrients conditions by varying the chlorophyll content in a cell such that only a fraction of phytoplankton growth ($\rho_{P_X}^{Chl}$) is dedicated to chlorophyll synthesis following *Geider et al.* [1996, 1997]:

$$\rho_{P_X}^{Chl} = \frac{\theta_{P_X}^{max} \mu_{P_X} P_X}{\alpha_{P_X} E Chl_X} \tag{17}$$

The rates of phytoplankton grazing by zooplankton and Z_L predation on Z_S (g_{XY}; d^{-1}) are represented by Holling-type III functions with the addition of an inhibition factor for Z_S grazing on P_L and Z_L grazing on P_S when an alternate food source is available:

$$g_{XY} = g_{XY}^{max} \frac{Y^2}{k_{XY} + Y^2} e^{-\psi_{XY}\omega} , \tag{18}$$

where g_{XY}^{max} (d^{-1}), k_{XY} ((mmol N $m^{-3})^2$) and ψ_{XY} ((mmol N $m^{-3})^{-1}$) are the maximum consumption rate, the half-saturation concentration and the inhibition coefficient for consumption of Y by X, respectively. Ω is the sum of alternate food source such that $\omega = P_S$ for Z_S grazing on P_L, $\omega = P_L + Z_S$ for Z_L grazing on P_S and $\omega = 0$ otherwise.

Nitrification (n; d^{-1}) is inhibited by light and low O_2 (Fennel et al., 2006, 2013):

$$\hat{n} = \left(1 - \hat{n}_{\max} \max\left[0, \frac{E - E_0}{k_E + E - E_0}\right]\right) \cdot \max\left[\left(\frac{O_2 - O_2^{th}}{k_{O_2} + O_2 - O_2^{th}}\right), 0\right], \tag{19}$$

whereas the remineralization parameters are modified by O_2 only (Fennel et al., 2013):

$$\hat{r}_{D_X} = r_{D_X} \cdot \max\left[\left(\frac{O_2 - O_2^{th}}{k_{O_2} + O_2 - O_2^{th}}\right), 0\right] \tag{20}$$

S3 References

Eppley, R. W.: Temperature and phytoplankton growth in the sea, Fish. Bull., 70(4), 1063–1085, 1972.

Evans, G. and Parslow, J. S.: A model of annual plankton cycles, Deep Sea Res. Part B. Oceanogr. Lit. Rev., 32(9), 759, doi:10.1016/0198-0254(85)92902-4, 1985.

Fennel, K., Wilkin, J., Levin, J., Moisan, J., O'Reilly, J. and Haidvogel, D.: Nitrogen cycling in the Middle Atlantic Bight: Results from a three-dimensional model and implications for the North Atlantic nitrogen budget, Global Biogeochem. Cycles, 20(3), GB3007, doi:10.1029/2005GB002456, 2006.

Fennel, K., Hu, J., Laurent, A., Marta-Almeida, M. and Hetland, R.: Sensitivity of hypoxia predictions for the northern Gulf of Mexico to sediment oxygen consumption and model nesting, J. Geophys. Res. Ocean., 118(2), 990–1002, doi:10.1002/jgrc.20077, 2013.

Geider, R., MacIntyre, H. and Kana, T.: Dynamic model of phytoplankton growth and acclimation:responses of the balanced growth rate and the chlorophyll a:carbon ratio to light, nutrient-limitation and temperature, Mar. Ecol. Prog. Ser., 148(1–3), 187–200, doi:10.3354/meps148187, 1997.

Geider, R. J., MacIntyre, H. L. and Kana, T. M.: A dynamic model of photoadaptation in phytoplankton, Limnol. Oceanogr., 41(1), 1–15, doi:10.4319/lo.1996.41.1.0001, 1996.

S4 Supplementary table and figures

Table S1. Parameters for the biological model.

Symbol	Value	Parameter description	Units
		Phytoplankton	
$\mu_{P_S}^0$	1.1629	Small phytoplankton maximum growth rate at 0°C	d^{-1}
$\mu_{P_L}^0$	1.1242	Large phytoplankton maximum growth rate at 0°C	d^{-1}
α_{P_S}	0.0405	Initial slope of the instantaneous growth rate vs light curve for P_S	$(W\ m^{-2})^{-1}d^{-1}$
α_{P_L}	0.0393	Initial slope of the instantaneous growth rate vs light curve for P_L	$(W\ m^{-2})^{-1}d^{-1}$
$k_{NO_3^-}$	0.5	NO_3^- half saturation concentration	mmol N m^{-3}
$k_{NH_4^+}$	0.5	NH_4^+ half saturation concentration	mmol N m^{-3}
$m_{P_S}^0$	0.2377	Phytoplankton mortality rate at 0°C for P_S	d^{-1}
$m_{P_L}^0$	0.1169	Phytoplankton mortality rate at 0°C for P_L	d^{-1}
$\theta_{P_S}^{max}$	0.0328	Maximum chlorophyll to carbon ratio for P_S	mgChl $(mg\ C)^{-1}$
$\theta_{P_L}^{max}$	0.0386	Maximum chlorophyll to carbon ratio for P_L	mgChl $(mg\ C)^{-1}$
$\theta_{C:N}^{P}$	6.625	Carbon to nitrogen ratio for phytoplankton	mmol C $(mmol\ N)^{-1}$
w_P	0.1	Phytoplankton sinking rate	m d^{-1}
$R_{O_2:NO_3^-}$	8.625	O_2 produced per mol of NO_3^- assimilated during photosynthesis	mmol O_2 $(mmol\ NO_3^-)^{-1}$
$R_{O_2:NH_4^+}$	6.625	O_2 produced per mol of NH_4^+ assimilated during photosynthesis	mmol O_2 $(mmol\ NH_4^+)^{-1}$
		Zooplankton	
$g_{Z_SP_S}^0$	6.6761	Maximum grazing rate at 0°C of Z_S on P_S	d^{-1}
$g_{Z_SP_L}^0$	6.6761	Maximum grazing rate at 0°C of Z_S on P_L	d^{-1}
$g_{Z_LP_S}^0$	3.33805	Maximum grazing rate at 0°C of Z_L on P_S	d^{-1}
$g_{Z_LP_L}^0$	1.1126	Maximum grazing rate at 0°C of Z_L on P_L	d^{-1}
$g_{Z_LZ_S}^0$	6.6761	Maximum consumption rate at 0°C of Z_L on Z_S	d^{-1}
$k_{Z_SP_S}$	0.5	Squared zooplankton grazing half saturation of Z_S on P_S	$(mmol\ N\ m^{-3})^2$
$k_{Z_SP_L}$	0.5	Squared zooplankton grazing half saturation of Z_S on P_L	$(mmol\ N\ m^{-3})^2$
$k_{Z_LP_S}$	0.5	Squared zooplankton grazing half saturation of Z_L on P_S	$(mmol\ N\ m^{-3})^2$
$k_{Z_LP_L}$	0.5	Squared zooplankton grazing half saturation of Z_L on P_L	$(mmol\ N\ m^{-3})^2$
$k_{Z_LZ_S}$	0.5	Squared zooplankton grazing half saturation of Z_L on Z_S	$(mmol\ N\ m^{-3})^2$
m_Z^0	0.0224	Zooplankton mortality at 0°C	$(mmol\ N\ m^{-3})^{-1}\ d^{-1}$
β_{Z_S}	0.75	Assimilation efficiency for Z_S	Dimensionless
β_{Z_L}	0.75	Assimilation efficiency for Z_L	Dimensionless
l_{BM}^0	0.0886	Zooplankton excretion rate due to basal metabolism at 0°C	d^{-1}
l_E^0	0.0886	Maximum rate of assimilation related excretion at 0°C	d^{-1}
$\psi_{Z_SP_L}$	3.010	Inhibition coefficient for Z_S grazing on P_L	$(mmol\ N\ m^{-3})^{-1}$
$\psi_{Z_LP_S}$	3.010	Inhibition coefficient for Z_L grazing on P_S	$(mmol\ N\ m^{-3})^{-1}$
		Nutrient and detritus	
n_{max}	0.2	Maximum nitrification rate	d^{-1}
E_0	0.0095	Radiation threshold for nitrification inhibition	W m^{-2}
k_E	0.1	Light intensity for half-saturated nitrification inhibition	W m^{-2}
τ	0.0023	Phytoplankton and small detritus aggregation	d^{-1}
r_{D_S}	0.4	Remineralization rate of D_S	d^{-1}
r_{D_L}	0.01	Remineralization rate of D_L	d^{-1}
w_{D_S}	0.1	Sinking rate of D_S	m d^{-1}
w_{D_L}	5.0	Sinking rate of D_L	m d^{-1}

$R_{O_2:NO_3^-}$	8.625	O_2 produced per mol of NO_3^- assimilated during photosynthesis	mmol O_2 (mmol NO_3^-)$^{-1}$
$R_{O_2:NH_4^+}$	6.625	O_2 produced per mol of NH_4^+ assimilated during photosynthesis	mmol O_2 (mmol NH_4^+)$^{-1}$

Table S2. ESMs ranking along the ACM open boundaries.

Ranked models			Ranks							
Name	ID	CMIP	Temp.	Salt.	Chl-a	NO3	$\overline{R}$	$\overline{R}_{bio}$	$\overline{R}_{phys}$	Overall
HadGEM2-ES	11	5	5	21	2	10	9.5	6.0	13.0	1
UKESM1-0-LL	30	6	20	4	9	5	9.5	7.0	12.0	2
MPI-ESM1-2-HR	28	6	17	1	20	1	9.7	10.5	9.0	3
CNRM-ESM2-1	22	6	9	3	4	23	9.7	13.5	6.0	4
MPI-ESM-MR	16	5	6	5	24	4	9.7	14.0	5.5	5
HadGEM2-CC	10	5	13	16	3	8	10.0	5.5	14.5	6
IPSL-CM6A-LR	26	6	4	20	11	6	10.2	8.5	12.0	7
GFDL-ESM2G	6	5	1	12	17	12	10.5	14.5	6.5	8
GFDL-ESM4	23	6	10	19	1	18	12.0	9.5	14.5	9
GISS-E2-R-CC	9	5	11	17	13	7	12.0	10.0	14.0	10
GISS-E2-1-G-CC	25	6	15	26	8	2	12.7	5.0	20.5	11
GISS-E2-1-G	24	6	16	27	7	3	13.2	5.0	21.5	12
IPSL-CM5A-MR	13	5	21	13	10	9	13.2	9.5	17.0	13
MIROC-ES2L	27	6	24	2	6	21	13.2	13.5	13.0	14
CanESM2	2	5	3	14	18	19	13.5	18.5	8.5	15
GFDL-ESM2M	7	5	8	15	5	27	13.7	16.0	11.5	16
IPSL-CM5A-LR	12	5	23	10	12	11	14.0	11.5	16.5	17
CanESM5	19	6	12	9	23	17	15.2	20.0	10.5	18
MPI-ESM-LR	15	5	19	6	26	13	16.0	19.5	12.5	19
NorESM2-LM	29	6	2	18	16	29	16.2	22.5	10.0	20
GISS-E2-H-CC	8	5	27	8	19	15	17.2	17.0	17.5	21
CNRM-CM5	5	5	26	11	14	28	19.7	21.0	18.5	22
CMCC-CESM	4	5	29	7	25	20	20.2	22.5	18.0	23
MRI-ESM1	17	5	25	29	15	14	20.7	14.5	27.0	24
CESM2	20	6	14	22	27	22	21.2	24.5	18.0	25
NorESM1-ME	18	5	7	23	29	26	21.2	27.5	15.0	26
CESM1-BGC	3	5	22	25	21	25	23.2	23.0	23.5	27
IPSL-CM5B-LR	14	5	28	28	22	16	23.5	19.0	28.0	28
CESM2-WACCM	21	6	18	24	28	24	23.5	26.0	21.0	29

Table S3. Correlation coefficients between ESM ranking on the shelf (Table 2) and along the ACM boundaries (Table S2). Correlations are calculated for individual variables and for the final ranking (with and without temperature) for the CMIP5, CMIP6 and all models.

Type	Variables				Total rank	Total rank w/o temp.
	Chlorophyll	Nitrate	Temperature	Salinity		
CMIP5	0.72	0.69	0.01	0.67	0.54	0.82
CMIP6	0.86	0.94	0.32	0.91	0.9	0.93
All models	0.8	0.81	0.05	0.81	0.74	0.87

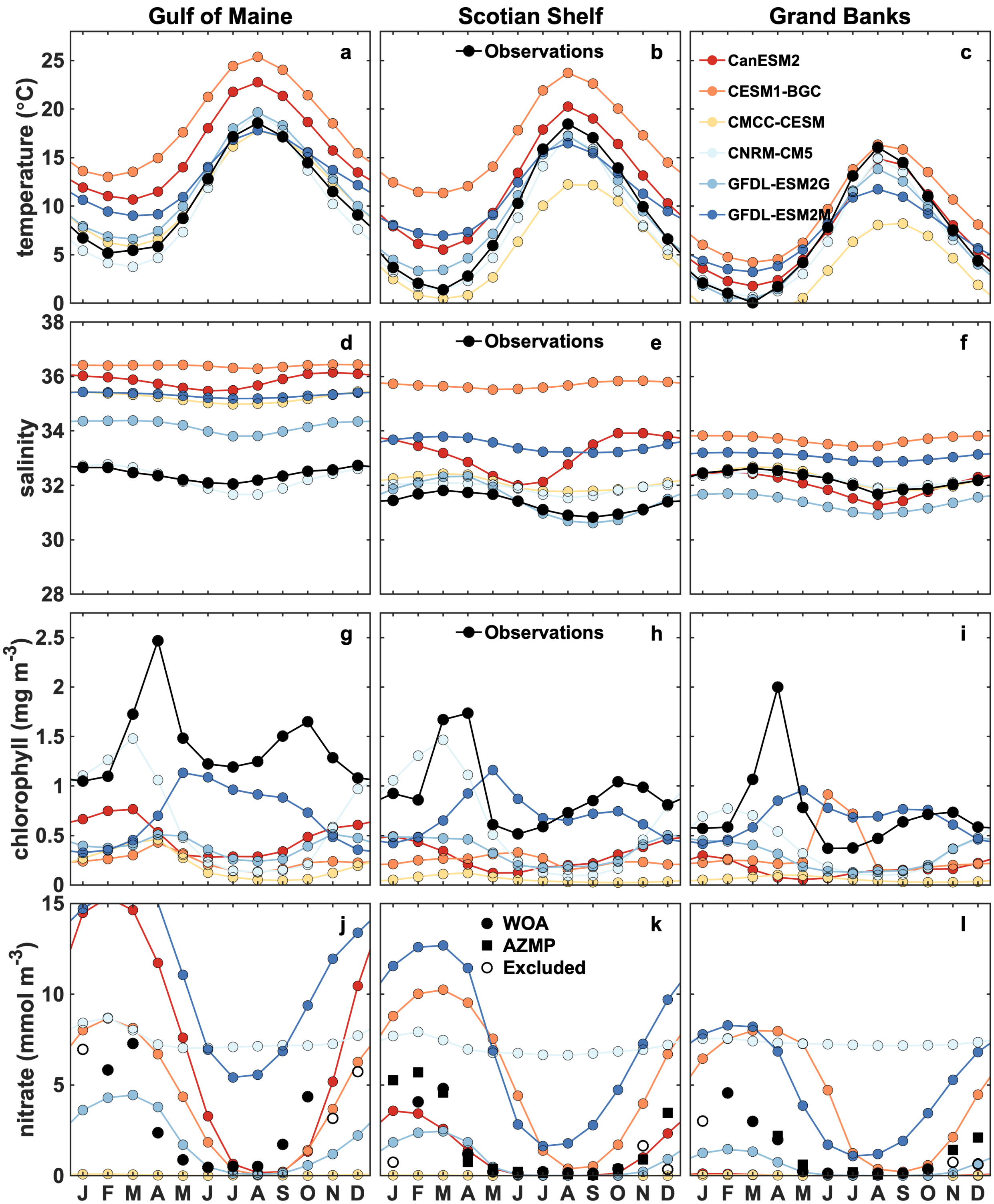

Figure S1. Comparison between observed (black) and simulated (models 2–7) area averaged surface temperature (a-c), salinity (d-f), chlorophyll (g-i) and nitrate (j-l) for the 3 ECS areas.

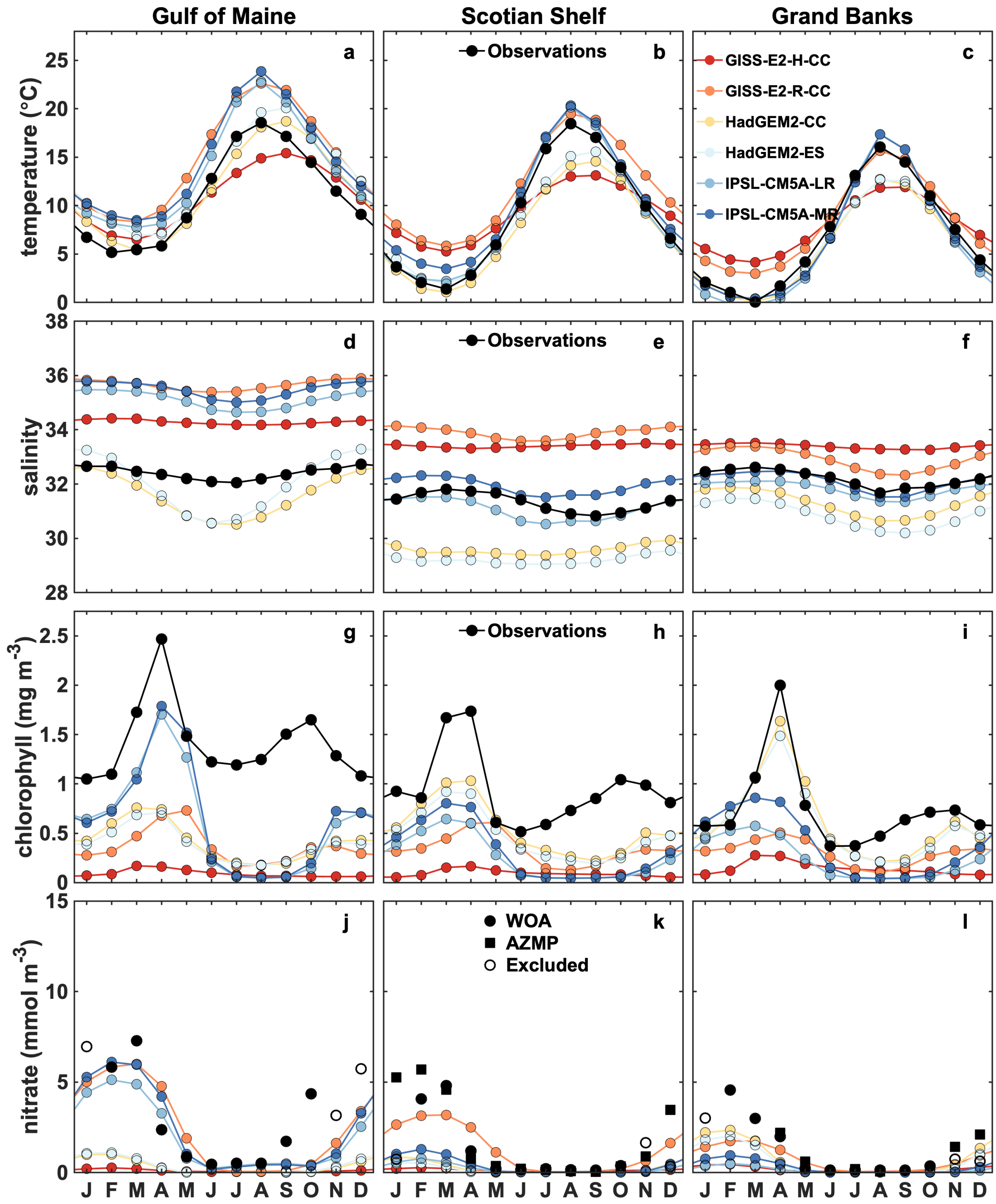

Figure S2. Comparison between observed (black) and simulated (ESMs 8–13) area averaged surface temperature (a-c), salinity (d-f), chlorophyll (g-i) and nitrate (j-l) for the 3 ECS areas.

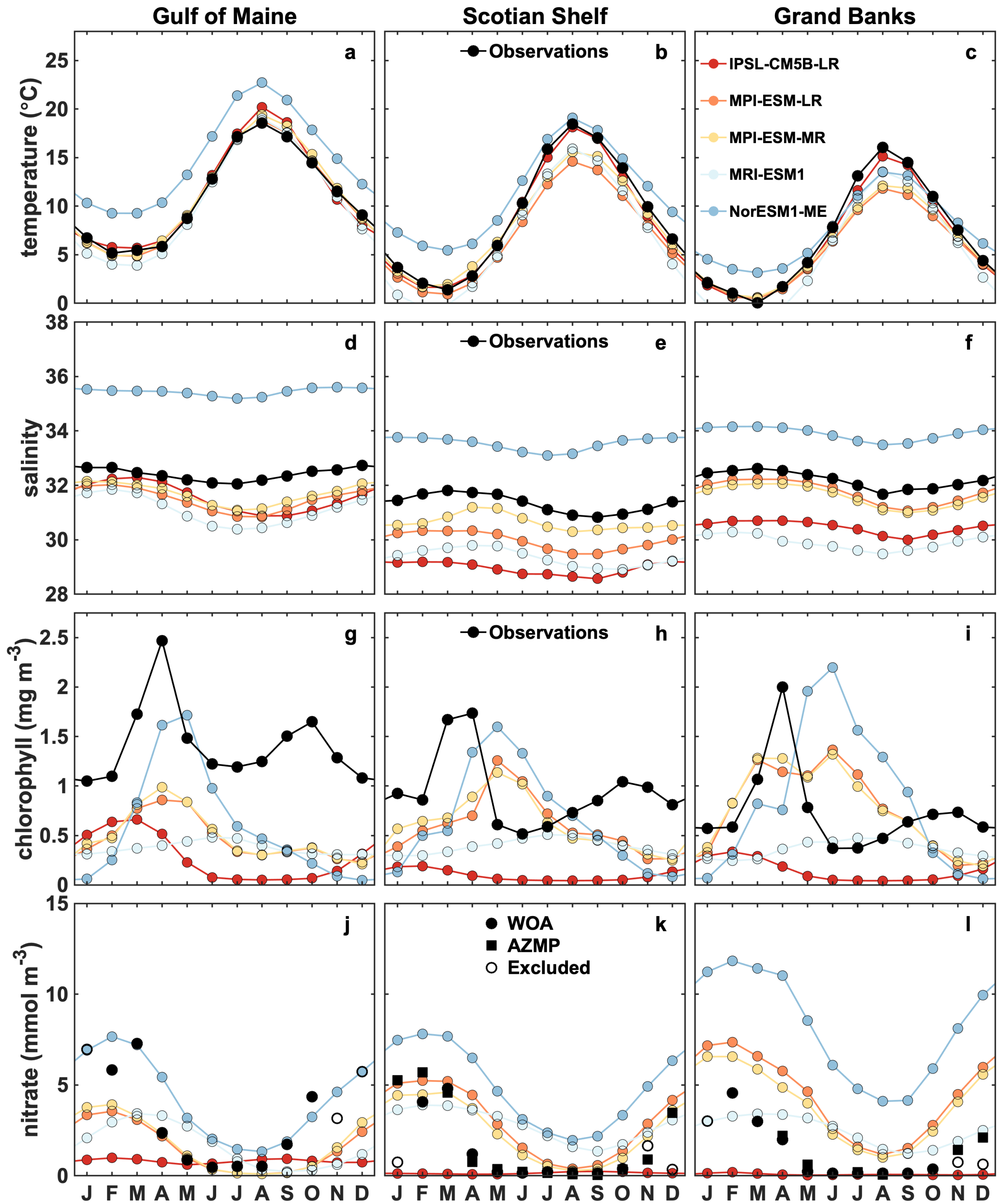

Figure S3. Comparison between observed (black) and simulated (ESMs 14–18) area averaged surface temperature (a-c), salinity (d-f), chlorophyll (g-i) and nitrate (j-l) for the 3 ECS areas.

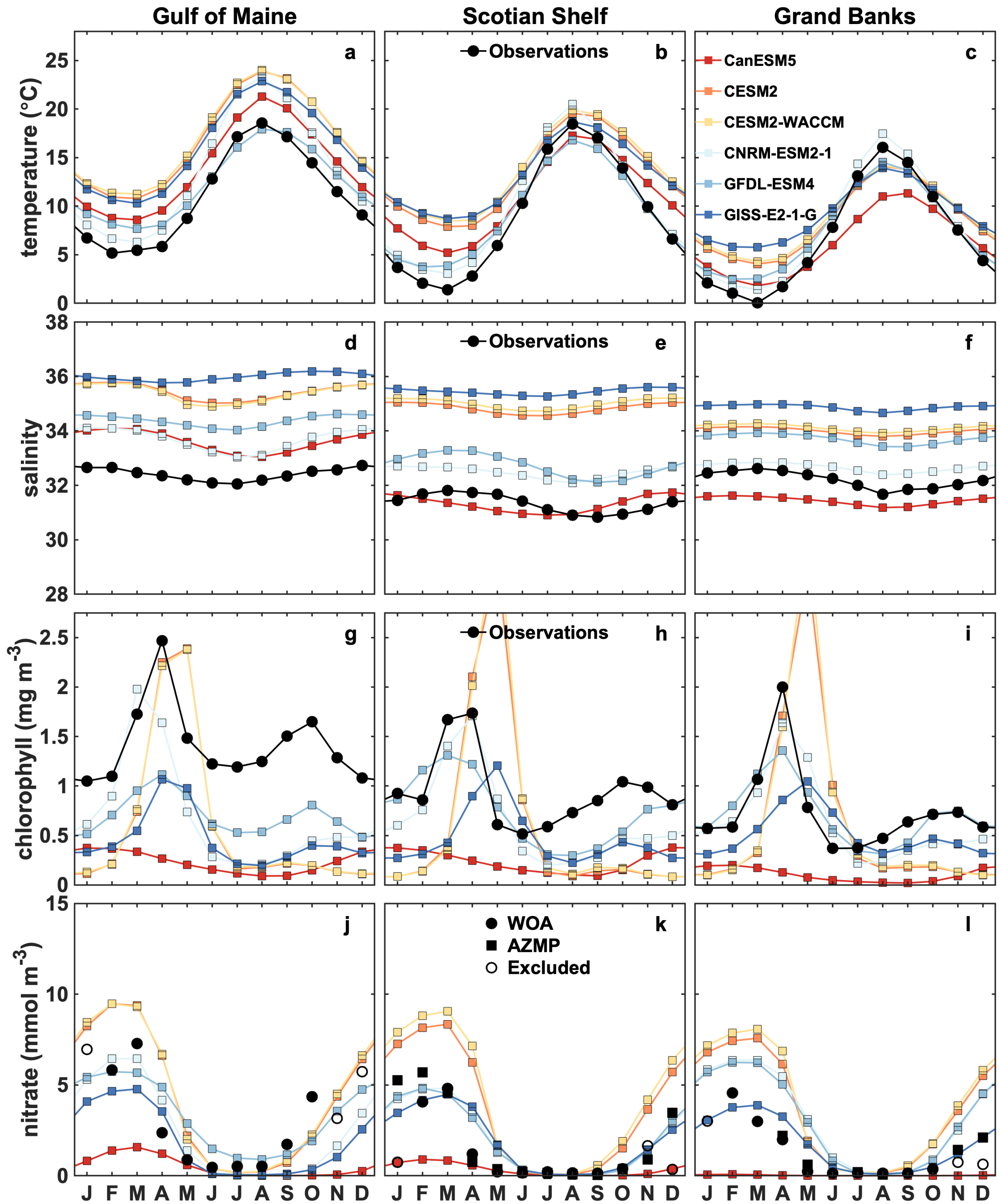

Figure S4. Comparison between observed (black) and simulated (ESMs 19–24) area averaged surface temperature (a-c), salinity (d-f), chlorophyll (g-i) and nitrate (j-l) for the 3 ECS areas.

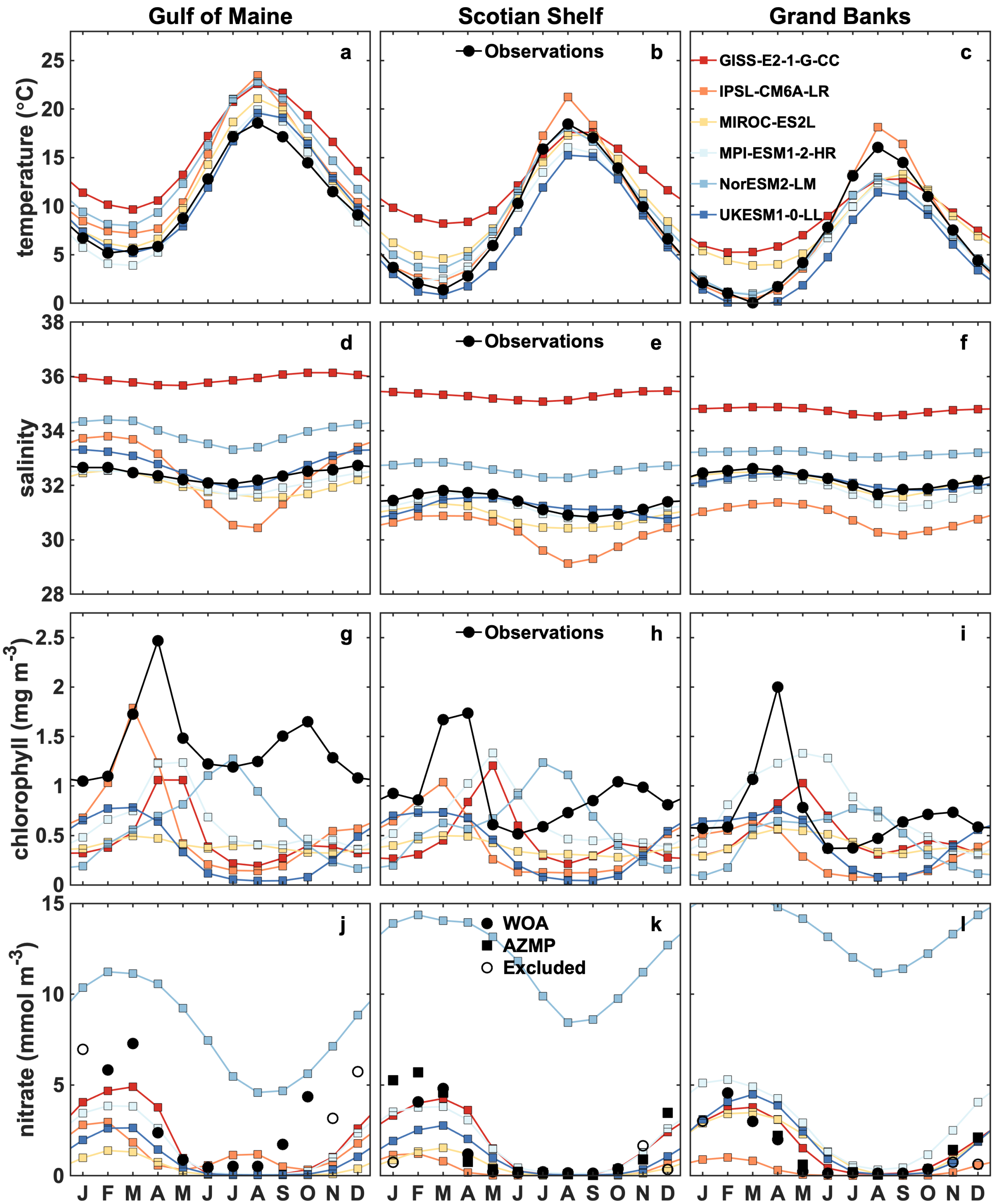

Figure S5. Comparison between observed (black) and simulated (ESMs 25–30) area averaged surface temperature (a-c), salinity (d-f), chlorophyll (g-i) and nitrate (j-l) for the 3 ECS areas.

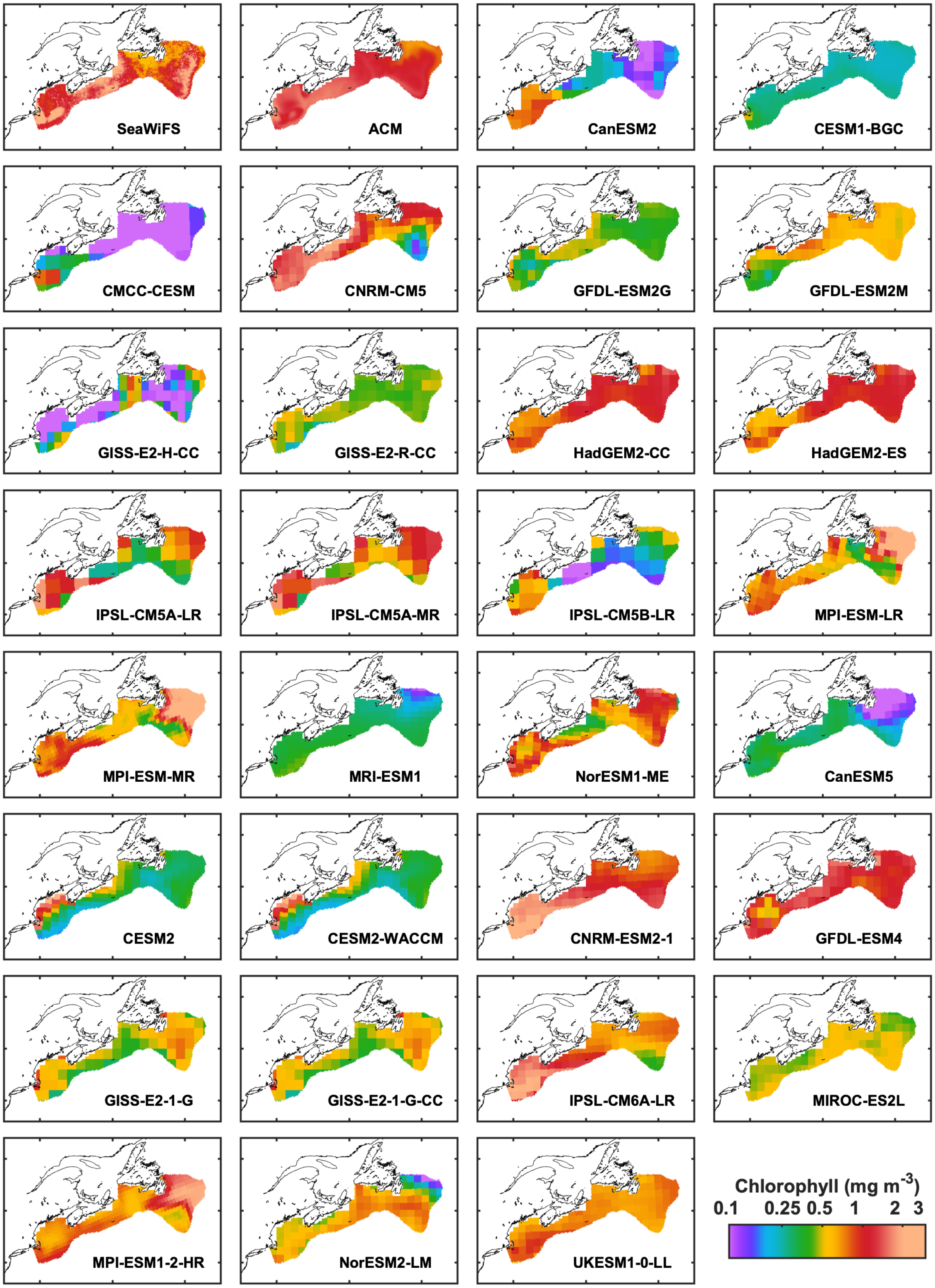

Figure S6. Comparison of SeaWiFS surface chlorophyll concentration in March with the simulated surface chlorophyll of the 30 models interpolated on the SeaWiFS grid.

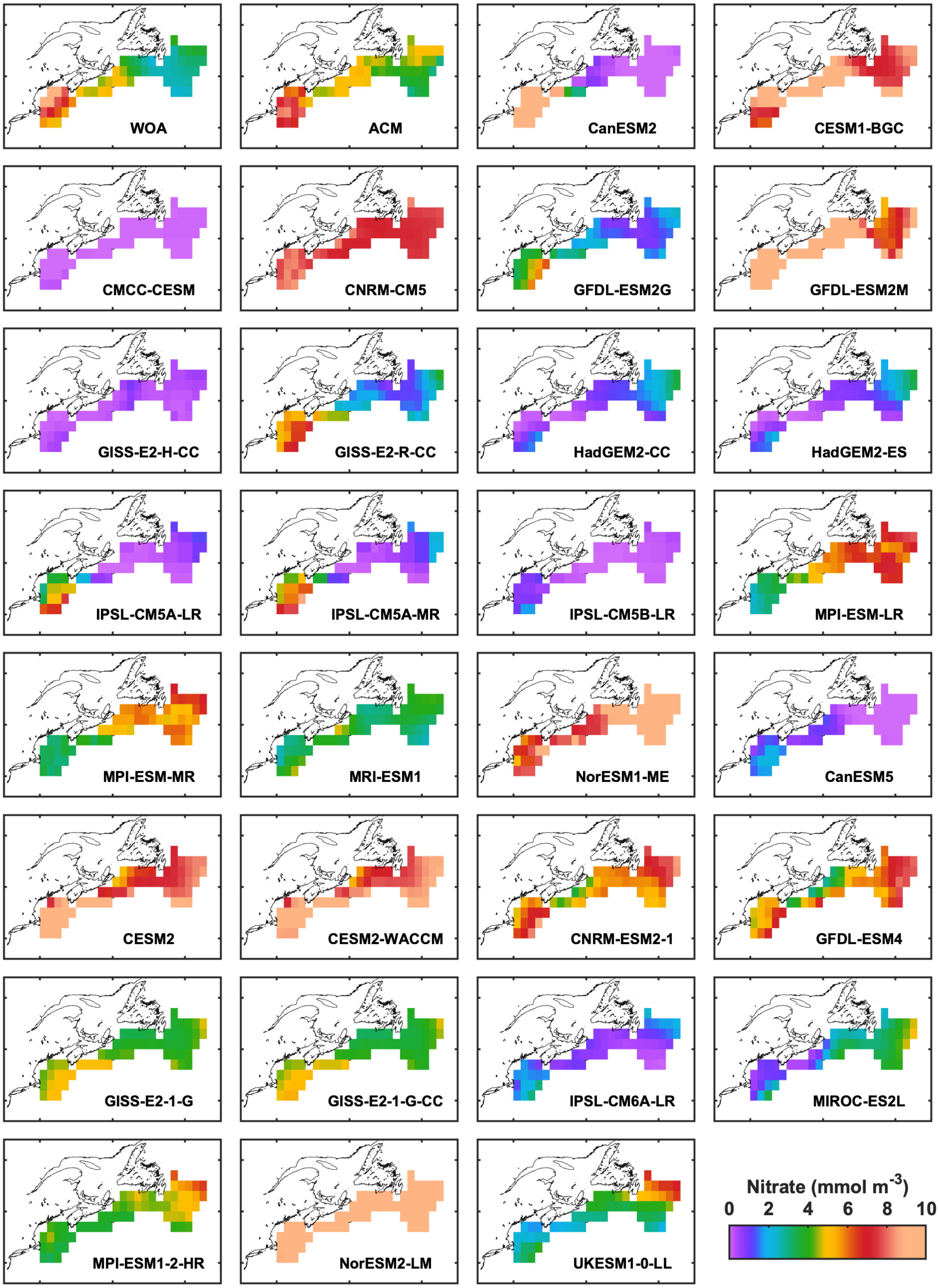

Figure S7. Comparison of WOA surface nitrate concentration in March with the simulated surface nitrate of the 30 models interpolated on the WOA grid.

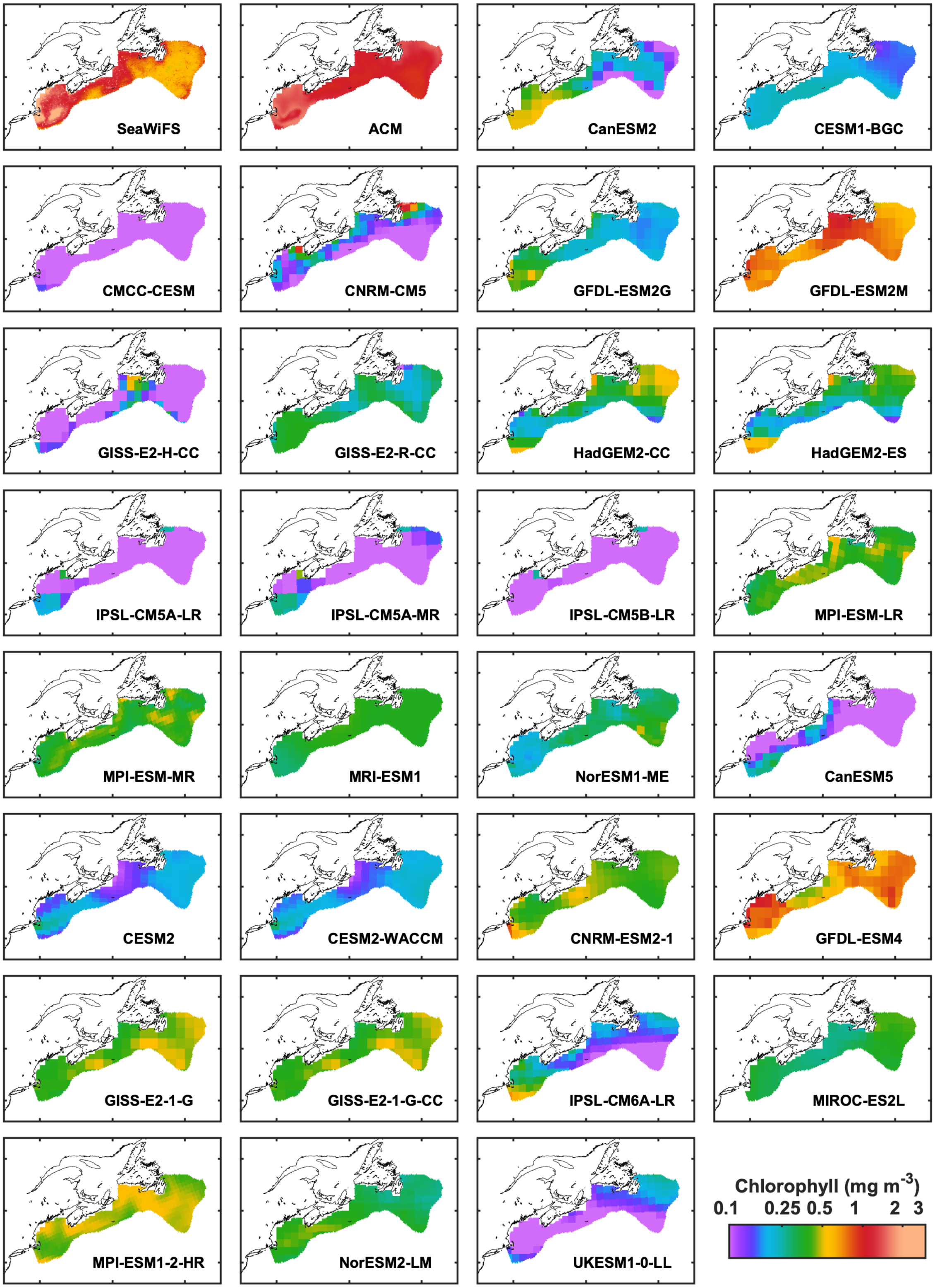

Figure S8. Same as Figure S6 but for October.

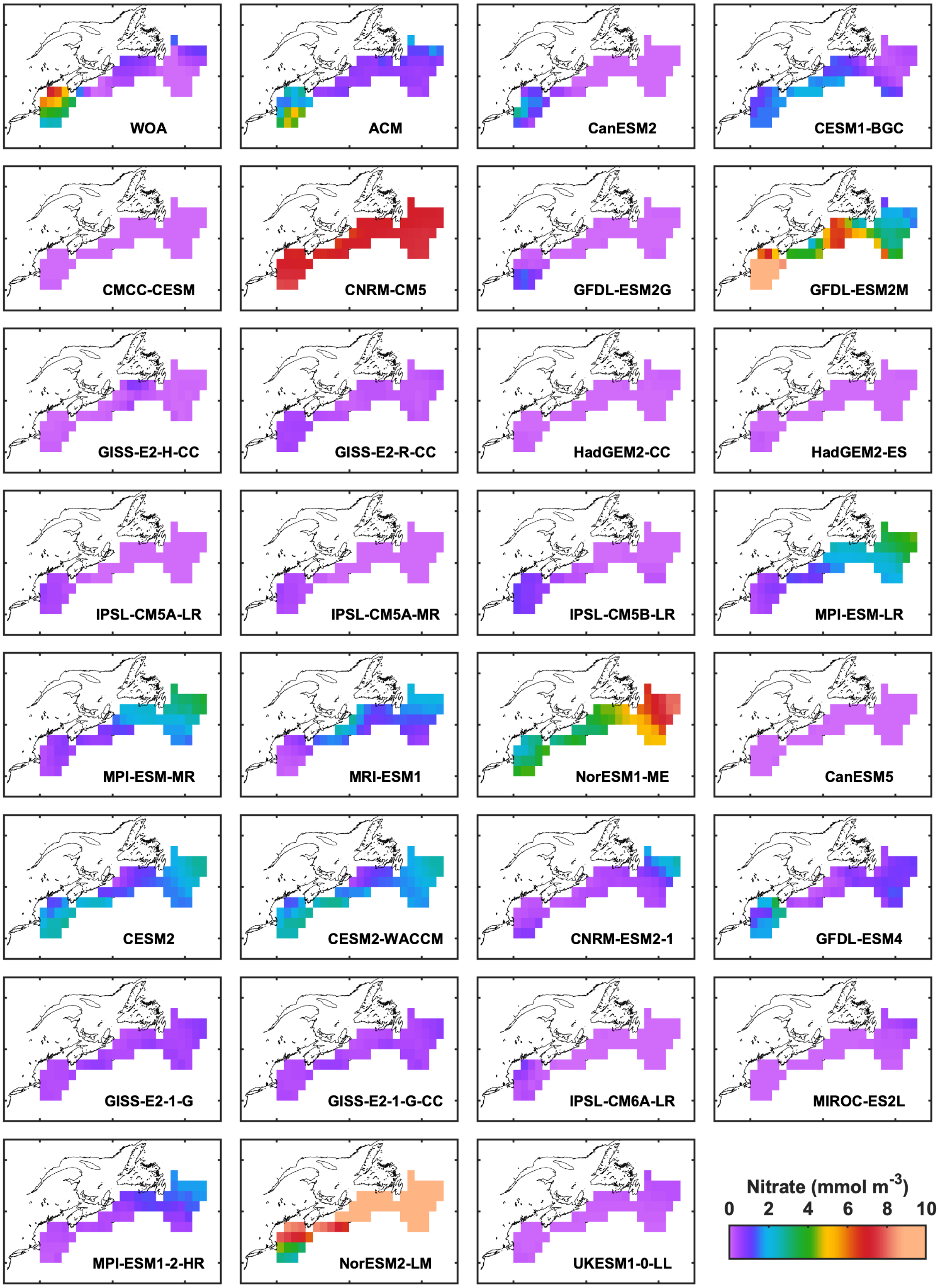

Figure S9. Same as Figure S7 but for October.

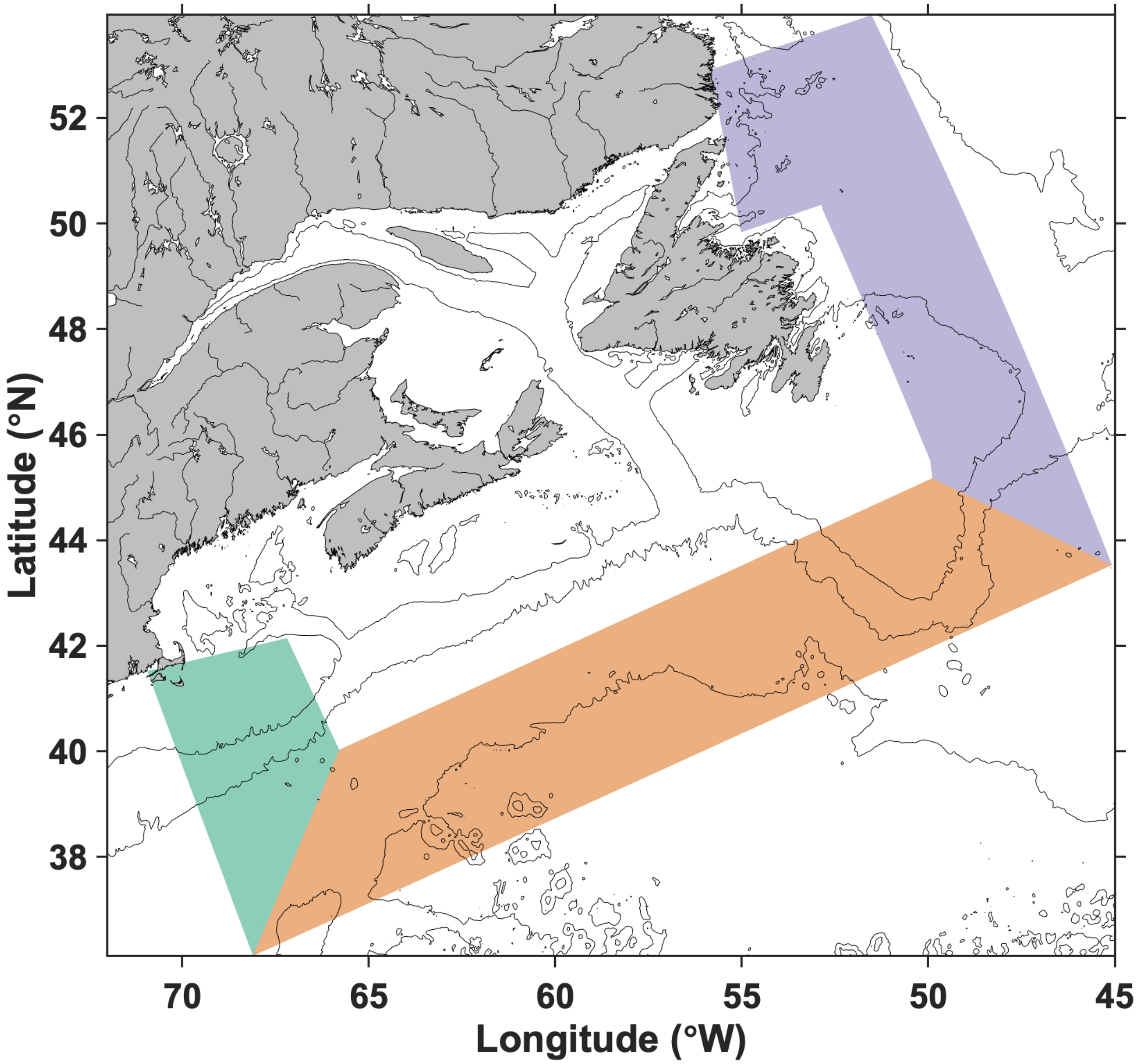

Figure S10. Location of the outer boundary area used to calculate model scores and ranking in Table S3. Individual boundaries are referred to as West (green), South (orange) and Northeast (purple).

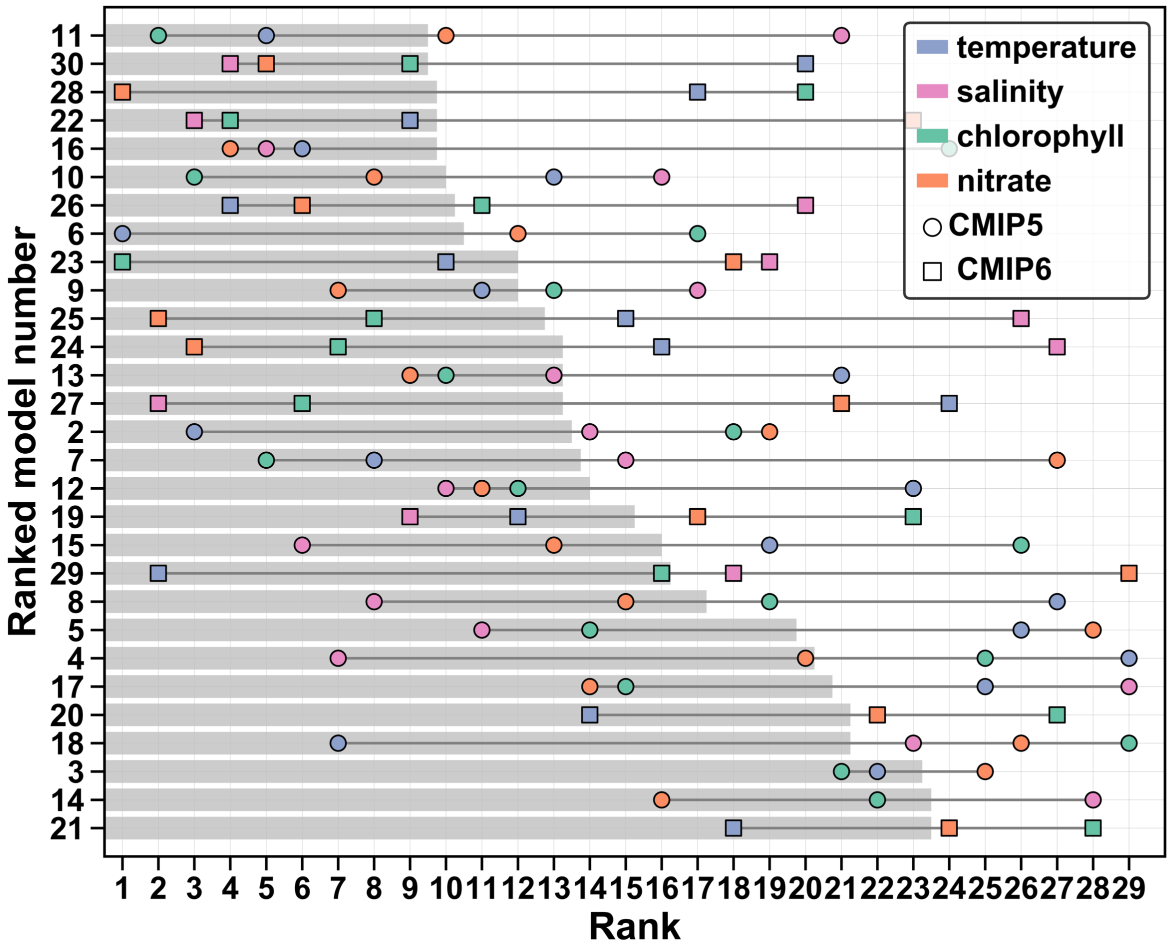

Figure S11. Model average (grey bars) and specific (dots) ranking. The final ranking is shown on the y-axis. Hidden coinciding ranks (models 3, 6, 14, 21 and 28) are provided in Table S2.

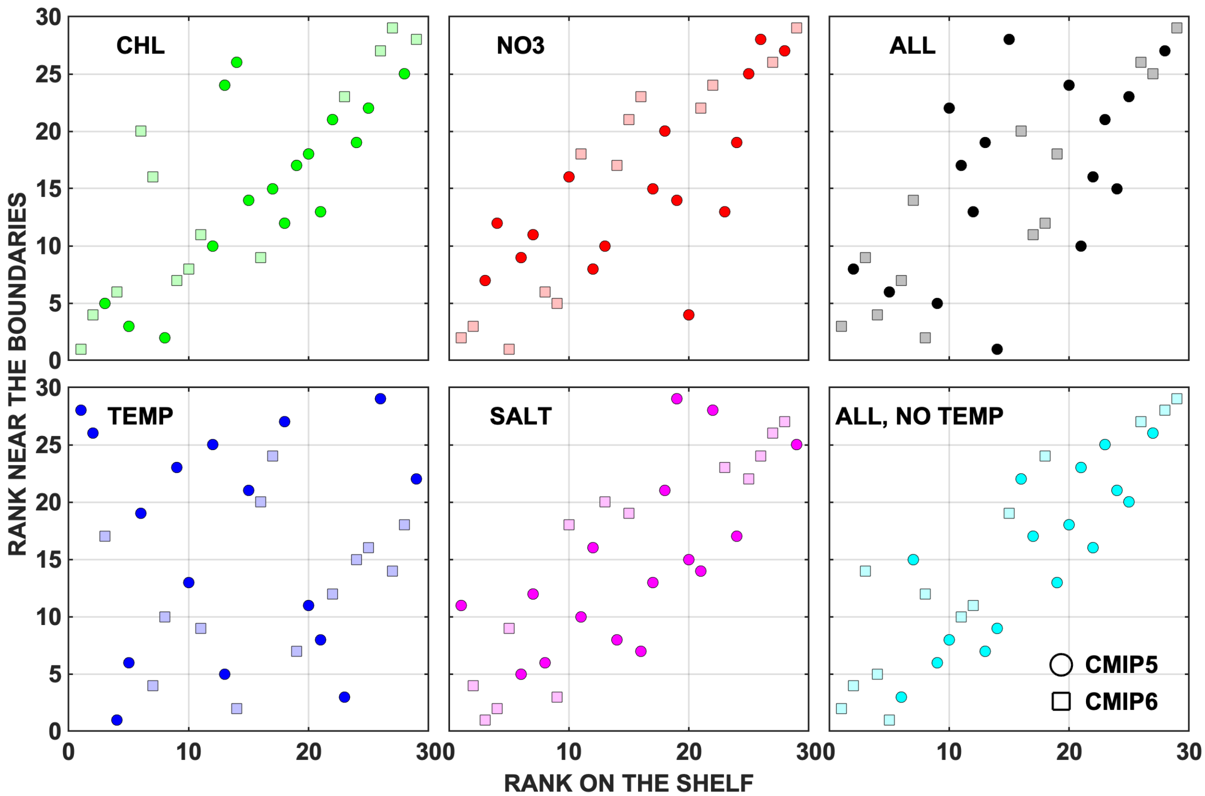

Figure S12. Relationships between ESM ranks on the shelf and along the ACM boundaries. Correlation coefficients are provided in Table S3.

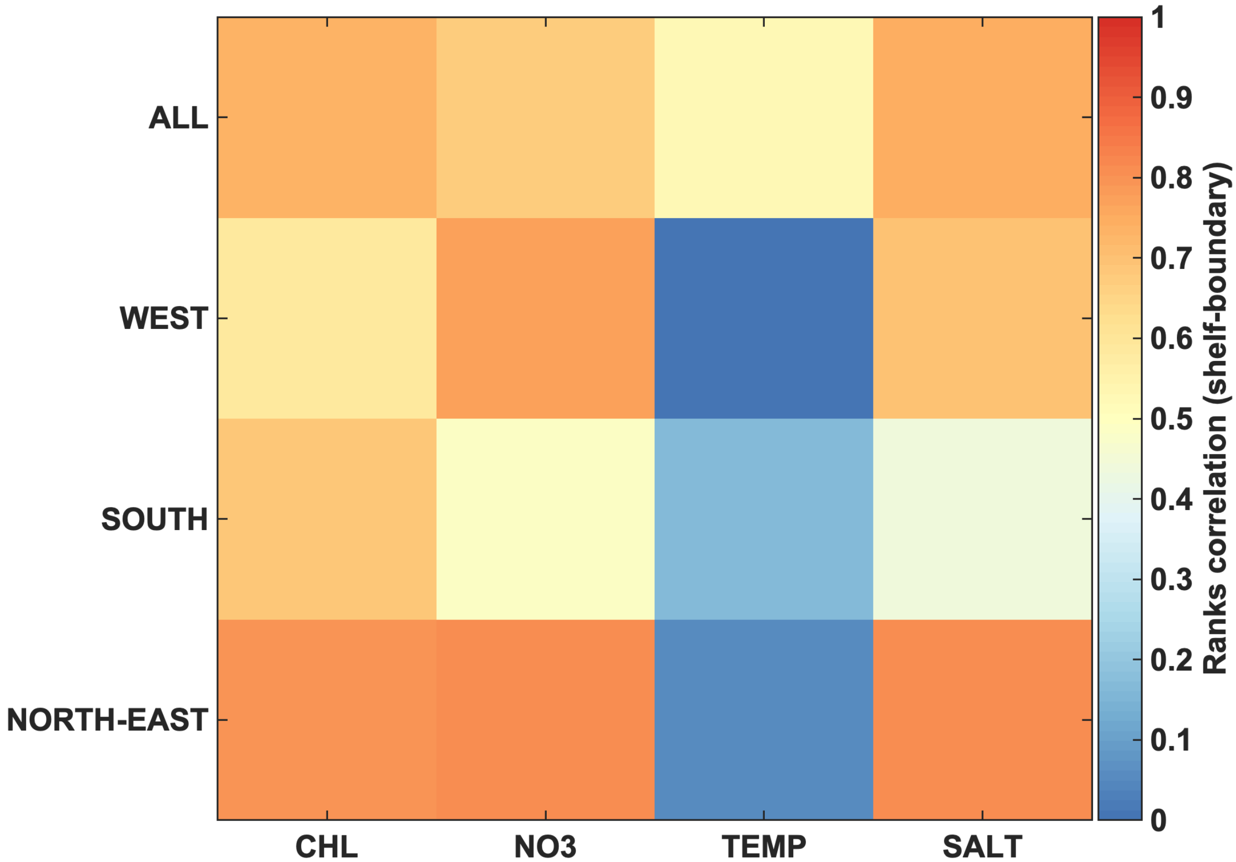

Figure S13. Correlation coefficients between ESM ranks on the shelf and along the ACM boundaries.

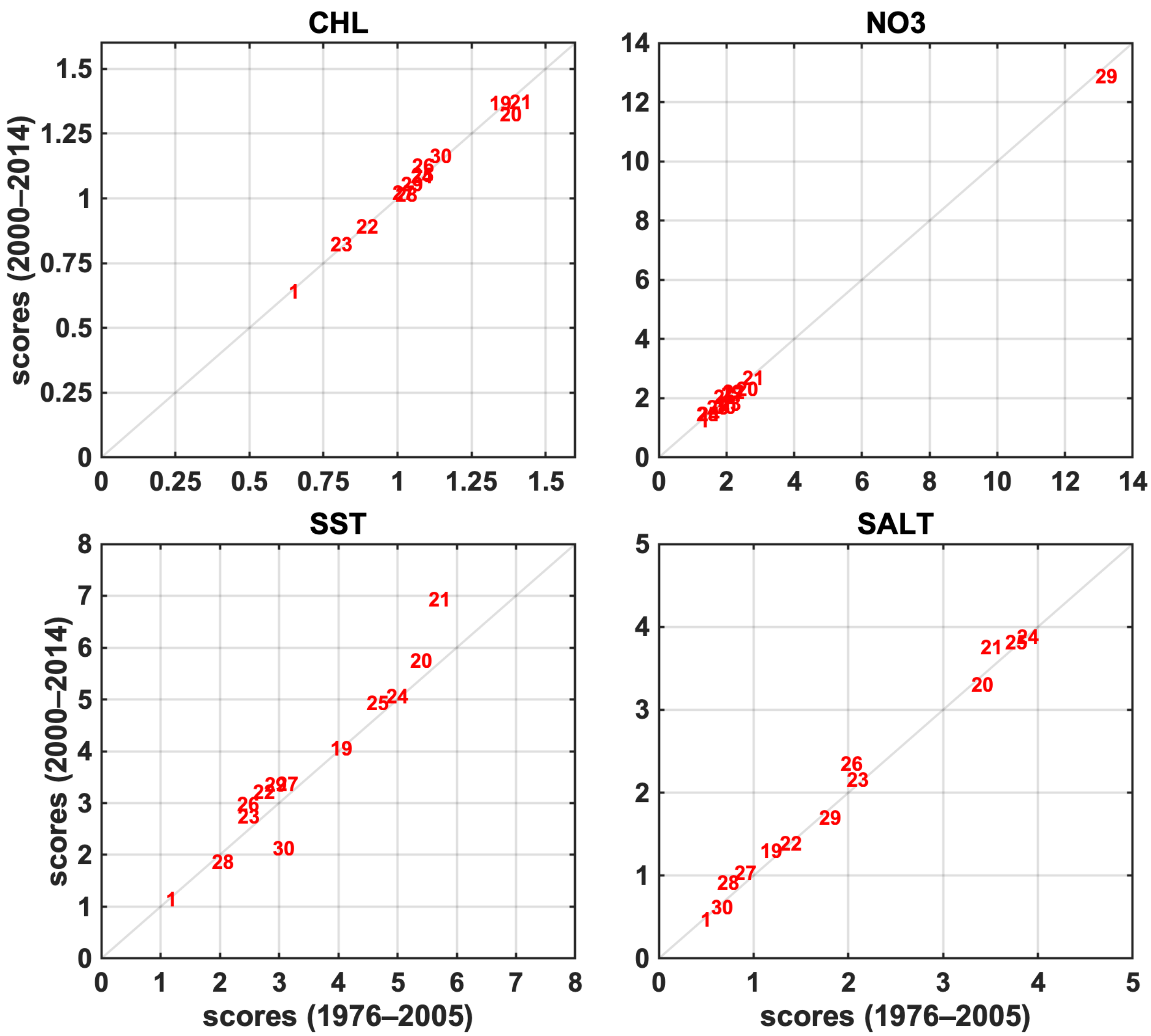

Figure S14. Relationships between scores from CMIP6 model climatologies averaged over 1976–2005 (x-axis) and 2000–2014 (y-axis). ACM (1) is indicated as reference.